Physics Letters B 279 (1992) 20–24
North-Holland

PHYSICS LETTERS B

Test for isotopic dependence of electron screening in fusion reactions ☆

S. Engstler, G. Raimann, C. Angulo, U. Greife, C. Rolfs, U. Schröder, E. Somorjai [1]
Institut für Physik mit Ionenstrahlen, Ruhr-Universität Bochum, W-4630 Bochum, FRG
and Institut für Kernphysik, Universität Münster, W-4400 Münster, FRG

B. Kirch and K. Langanke
Institut für Theoretische Physik, Universität Münster, W-4400 Münster, FRG

Received 13 November 1991

The fusion reactions ^{6}Li(p, α)^{3}He, ^{6}Li(d, α)^{4}He and ^{7}Li(p, α)^{4}He have been studied over the CM energy range $E=10$–1004 keV. The effects of electron screening have been observed in all three reactions exhibiting the same enhancements for a given experimental technique. The deduced values for the screening potential energy are significantly larger compared to values calculated via the united atom test. This difference between observation and expectation is not understood at present.

The cross section $\sigma(E)$ of fusion reactions drops steeply at energies E far below the Coulomb barrier. To extrapolate the data to the energies of hydrostatic burning phases in various astrophysical scenarios (essentially to zero energy), it is advantageous to transform the cross section into the astrophysical $S(E)$ factor defined by the relation [1]

$$\sigma(E)=S(E)E^{-1}\exp(-2\pi\eta)\,, \qquad (1)$$

where $2\pi\eta=31.29Z_1Z_2(\mu/E)^{1/2}$ is the Sommerfeld parameter (Z_1 and Z_2 are the charge numbers of the interacting nuclides, μ is the reduced mass in amu, E is the CM energy in keV). In the case of reactions involving light nuclides, the $S(E)$ factor often varies slowly with energy.

In eq. (1) it is assumed that the Coulomb potential of the target nucleus and projectile is that resulting from bare nuclei, and thus the potential would extend to infinity. However, for nuclear reactions studied in the laboratory, the target nuclei are usually in the form of neutral atoms or molecules. The atomic (or molecular) electron cloud surrounding the target nucleus acts [2] as a screening potential: an incoming charged projectile experiences no repulsive Coulomb force until it penetrates the electron cloud; thus, the projectile sees a reduced Coulomb barrier. This in turn leads to a higher cross section, $\sigma_s(E)$, than would be the case for bare nuclei, $\sigma_b(E)$, with an enhancement factor [2]

$$f(E)=\sigma_s(E)/\sigma_b(E)\simeq\exp(\pi\eta U_e/E)\,, \qquad (2)$$

where U_e is the constant electron screening potential energy (e.g. $U_e\simeq Z_1Z_2e^2/R_a$, with R_a an atomic radius). Note that $f(E)$ increases exponentially with decreasing incident energy. For energy ratios $E/U_e\geqslant 1000$, shielding effects are negligible, and laboratory experiments can be regarded as essentially measuring $\sigma_b(E)$. However, for $E/U_e\leqslant 100$, shielding effects cannot be neglected and become important for understanding low-energy data. Relatively small enhancements from electron screening at energy ratios $E/U_e\simeq 100$ can cause significant errors [3] in the extrapolation of cross sections to lower energies, if the curve of the cross section is forced to follow the trend of the enhanced cross sections, without correction for the screening. Notice that for astro-

☆ Supported in part by the Landesamt Nordrhein-Westfalen (IVA5-10600387), the Deutsche Forschungsgemeinschaft (Ro429/18-2 and Ro429/21-1), and the Comision Interministerial de Ciencia y Tecnologia (AEN90-0932).

[1] Permanent address: Institute of Nuclear Research of the Hungarian Academy of Sciences, Debrecen, Hungary.

physical and other applications (stellar and fusion plasmas) the value of $\sigma_b(E)$ must be known because the screening in these applications is quite different from that in laboratory nuclear reaction studies, and $\sigma_b(E)$ must be explicitly included for each situation [2]. Recent low-energy studies of ^{3}He(d, p)^{4}He have shown [4] clearly such screening effects for the first time, as well as their dependence on the aggregate state of the target. Theoretical analyses [5] suggest that a Born–Oppenheimer approximation – based on phenomenological and/or approximate screening potentials – cannot describe these data; thus a dynamical treatment may be needed. Clearly, a thorough understanding of screening effects requires additional efforts in theory as well as in experiment, where improved low-energy data for other fusion reactions are needed. Such data are reported here for the fusion reactions [6–20] ^{6}Li(p, α)^{3}He, ^{6}Li(d, α)^{4}He and ^{7}Li(p, α)^{4}He using different aggregate states of the target (solid and gas targets for each reaction). Since the screening potential energy U_e [fit parameter in eq. (2)] depends only on the details of the electron clouds, there should be – in this simple model [2] – no isotopic effects on U_e and the extracted values for U_e of each target aggregate state should be identical in all three fusion reactions. A test of this hypothesis is reported here for the first time (for details, see refs. [21, 22]).

The experimental equipment, setup, and procedure are similar to those described previously. Briefly, the accelerators at Münster (350 kV) and Bochum (100 kV, 400 kV and 4 MV) provided p, d, ^{6}Li and ^{7}Li ion beams in the CM energy range $E=10$–1004 keV. The absolute ion beam energy of the accelerators is known to high precision leading to a maximum error in cross section of ±6%.

In the case of Li ion beams, a windowless gas target system was used. The beam entered the target chamber through five apertures of high pumping impedance and was stopped in a 2 W or 20 W beam calorimeter. For the measurement of angular distributions, excitation functions, and absolute cross sections at $E=30$–1004 keV, a disc-shaped target chamber was used with seven well-collimated Si detectors placed at $\theta_{lab}=30°$–135° (distance to the target center $d=17.5$ cm). The measurement of excitation functions was also carried out at $E=10$–92 keV in close geometry using a rectangular target chamber with a pair of Si detectors (covered with Ni foils to stop elastic scattered Li ions) at opposite sides to the beam axis ($d=0.9$ cm). A NE102A plastic scintillator with a cylindrical hole at its center surrounded the target chamber and was used to detect the contributions of cosmic rays. The hydrogen gas pressure in the target chamber [enrichment $H_2=99.99\%$ and $D_2=99.9\%$; pressure $p(H_2)=1.0$ mbar and $p(D_2)=0.5$ mbar] was measured with a Baratron capacitance manometer to an accuracy of ±0.1%. The number of incident projectiles was determined to an accuracy of ±2.5% with the use of the beam calorimeters. The calorimeter was placed at such a distance from the gas target that angle straggling of the ions in the gas resulted in a beam profile smaller than the 200 mm^2 active area of the calorimeter.

In the case of hydrogen ions and LiF solid targets, two sets of experiments were carried out. Firstly, the measurement of angular distributions for ^{6}Li(p, α)^{3}He and ^{7}Li(p, α)^{4}He at $E=26$–171 keV (350 kV Münster accelerator) was performed in an ORTEC scattering chamber with a 1.1 μg/cm^2 thick LiF target on a Ta backing (Li = natural isotopic composition) at the center of the chamber and six Si detectors placed at $\theta_{lab}=60°$–160° ($d=21$ cm). Secondly, excitation functions for all three fusion reactions were obtained at $E=10$–85 keV (100 kV Bochum accelerator) using a setup, in which the beam passed first through a 1.3 cm diameter Ta collimator and was focussed then on the target into a spot of about 2.5 cm diameter. The LiF target (with direct water cooling applied to the backing) was of natural Li [for ^{7}Li(p, α)^{4}He] or of 95% enriched ^{6}Li [for ^{6}Li(p, α)^{3}He]. It was oriented with its normal antiparallel to the beam direction. Due to high sputtering rates at low energies, the LiF targets were fabricated with a thickness larger than 1 mg/cm^2. A liquid-nitrogen cooled in-line copper tube (65 cm length, 3 cm inner diameter) extended from the Ta collimator to within about 2 cm of the target. With this tube no carbon buildup on the target was observed ($p=5\times10^{-7}$ mbar). The reaction products were observed with four Si detectors (each of 600 mm^2 active area) positioned at $\theta_{lab}=130°$ around the beam axis ($d=4.9$ cm) leading to a total solid angle of 0.92 sr; the detectors were electrically isolated from the cylindrical target chamber and were covered with Ni foils to stop the intense flux of elastically scattered ions. The target together

with the target chamber and the Ni foils formed the Faraday cup for beam integration. The target chamber was surrounded again by the NE102A plastic scintillator. For the measurement of in-situ target stoichiometry, the target end-station was sealed with two valves (maintaining a pressure of 1×10^{-4} mbar) and transported from the 100 kV accelerator to the 400 kV and 4 MV accelerators. Due to problems of beam-induced target stoichiometry, the absolute scales of the solid target data have been normalized to previous results at overlapping energies.

The effective energy E within the target was derived from the incident energy of the ion beam, the energy loss of the beam in the target, and the effects of molecular ions (H_2^+ and H_3^+), if applicable.

The observed angular distributions in CM coordinates are expressed in terms of Legendre polynomials,

$$W(\theta,E)=\sum_k a_k(E)Q_kP_k(\cos\theta)\,, \qquad (3)$$

where Q_k are the attenuation coefficients. In the case of the ^{6}Li(d, α)^{4}He and ^{7}Li(p, α)^{4}He reactions, $W(\theta, E)$ is symmetrical around $\theta=90°$; one finds $a_4(E)\simeq0$ and $a_2(E)$ increasing monotonically with E, with a change of sign at about 80 keV. In the case of ^{6}Li(p, α)^{3}He, $W(\theta, E)$ is dominated by the $a_1(E)$ coefficient increasing monotonically with E and exhibiting a change in sign also at about 80 keV; the $a_2(E)$ coefficient is small in comparison. The clear change in sign of the dominant a_k coefficients at low energies is reported for the first time. The results are in excellent agreement with previous work in the overlapping energy regions.

With $U_e\simeq240$ eV for the Li+H system [2] one expects a negligible enhancement of 0.8% due to electron screening for $E\geqslant100$ keV. Thus, the abundant data for LiF solid targets (fig. 1b) have been fitted with the polynomial expansion

$$S_b(E)=a+bE+cE^2+dE^3 \qquad (4)$$

at energies $E\geqslant100$ keV to obtain approximately the energy dependence of $S_b(E)$ for bare nuclei. The results (table 1) are in fair agreement, (5–10)%, with available theoretical analyses of the data based on the R-matrix formalism [23] (for ^{6}Li+d), resonating group method [24] (for ^{6}Li+p), and the DWBA [22] (for ^{7}Li+p); it should be noted that none of these calculations exhibits an enhancement in $S_b(E)$

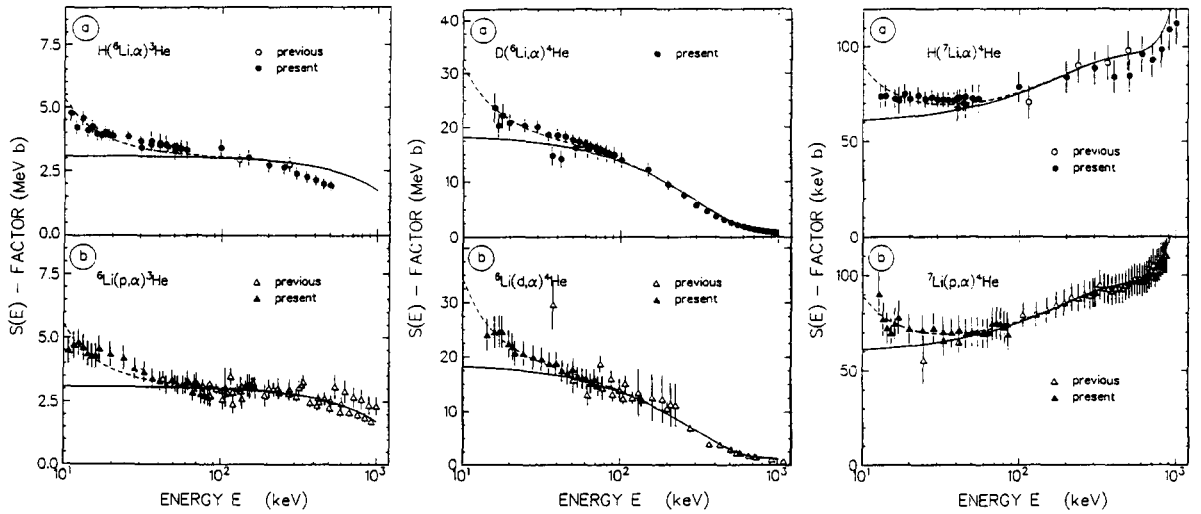

Fig. 1. Previous [6–20] and present data for the $S(E)$ factor of the ^{6}Li(p, α)^{3}He, ^{6}Li(d, α)^{4}He, and ^{7}Li(p, α)^{4}He reactions are shown as obtained with (a) molecular hydrogen targets (inverse kinematics) and (b) LiF solid targets (normal kinematics). The solid curve for each reaction corresponds to a polynomial expansion (fit) of the abundant LiF solid target data at $E\geqslant100$ keV; the curve represents approximately the case of bare nuclei. Except for absolute normalization (see text), the energy dependence of the polynomial expansion was assumed to be valid also for the (sparer) gas target data at $E\geqslant100$ keV. The dashed curve represents the inclusion of the effects of electron screening.

Table 1
Polynomial expansion $S_b(E) = a + bE + cE^2 + dE^3$ at $E = 0.1$–1.0 MeV.

Coefficient [a]	^{6}Li(p, α)^{3}He	^{6}Li(d, α)^{4}He	^{7}Li(p, α)^{4}He
a (MeV b)	2.86	17.4	0.0587
b (b)	−0.855	−54.2	0.191
c (MeV^{-1} b)	−0.411	61.7	−0.352
d (MeV^{-2} b)	-	−23.9	0.234
χ^2	1.0	0.7	0.06

[a] The coefficients have to be finally multiplied by a factor 1.08, 1.09, and 1.01 for the reactions ^{6}Li(p, α)^{3}He, ^{6}Li(d, α)^{4}He, and ^{7}Li(p, α)^{4}He, respectively (table 2).

at energies below 100 keV. Taking into account the present data for molecular gas targets at $E \geq 100$ keV and averaging the absolute scales of these data with previous data with the aid of the polynomial expansion, the resulting overall normalization factors are given in table 2. The resulting "corrected" data from previous and present work are illustrated in fig. 1a for molecular hydrogen targets (inverse kinematics) and in fig. 1b for LiF solid targets (normal kinematics). The errors shown represent total uncertainties. Good agreement is noted in the energy dependence of all data, except for ^{6}Li + p at $E = 300$–500 keV.

The data for all three fusion reactions exhibit an enhancement at low energies due to the effects of electron screening. A fit using eq. (2) (with U_e as free parameter) leads to results summarized in table 2 and shown as dashed curves in fig. 1. For the approximations used here (in particular the assumed $S_b(E)$ form at $E \leq 100$ keV), several conclusions may be drawn:

(i) For each set of experimental techniques (gas and solid targets) the deduced values of the screening potential energy U_e for all three reactions are identical within experimental error; thus, there appears to be no evidence for isotopic effects on electron screening, as expected from the simple model [2].

(ii) The U_e values for LiF solid targets (weighted average is 420 ± 120 eV) are somewhat higher compared to those for molecular hydrogen targets (weighted average is 350 ± 80 eV). This observation is similar to the report for the ^{3}He(d, p)^{4}He reaction [4], where the observed difference of $\Delta U_e \simeq 60$ eV between atomic and molecular targets was explained to a large extent by the effects of Coulomb explosion. In the present case the situation is more complicated due to solid state effects (such as chemical shifts and formation of image charges) and thus no attempt was made to explain the difference in the above U_e values.

(iii) The U_e values derived from both experimen-

Table 2
Screening potential energy U_e [a] and overall normalization k [b].

Reaction	Molecular hydrogen target		χ^2	LiF solid target		χ^2
	U_e [c] (eV)	k		U_e [c] (eV)	k [d]	
^{6}Li(p, α)^{3}He	440 ± 150	0.93	1.8	470 ± 150	1.08	0.6
^{6}Li(d, α)^{4}He	330 ± 120 [e]	0.93 [e]	0.9	380 ± 250	1.08	0.1
^{7}Li(p, α)^{4}He	300 ± 160	0.99	0.6	300 ± 280	1.01	0.1

[a] Assuming an $S_b(E)$ factor for bare nuclei as given in table 1.
[b] Correction factor to normalize data of atomic and molecular targets to the same absolute scale at $E \geq 100$ keV.
[c] Errors quoted correspond to one standard deviation.
[d] The normalization factor also applies to the previous measurement [9] using molecular hydrogen targets (open data points in fig. 1a).
[e] Fit to data at $E \leq 0.5$ MeV only.

tal techniques are significantly larger than the estimated value of $U_e \simeq 240$ eV for the simple Coulomb model; considerations of electron binding energies (i.e., united atom test with $U_{atom} = 15.7Z^{7/3}$ eV) result in $U_e \simeq 200$ eV. The difference between the observed and expected U_e values – also reported in the case [4] of ^{3}He(d, p)^{4}He – is not understood at present.

The authors would like to thank H.W. Becker, G. Blüge, A. Krauss, and H.P. Trautvetter for many discussions, and H. Baumeister, K. Brand, H. Ebbing, A. Gottdang, B. Hippert, A. Mann, and H. Schulte for technical assistance. We are also grateful to M. Berheide, A. Gardberg, U. Giesen, C. Iliadis, N. Mayer, K. Neldner, G. Roters, T. Schange, S. Schmidt, S. Seuthe, A. Stefan, R. Timmermann, M. Topheide, K. Wolke, and S. Wüstenbecker for help during the course of the experiments. We also thank C.A. Barnes and J.F. Harmon for fruitful discussions and R.W. Kavanagh for comments on the manuscript.

References

[1] C. Rolfs and W.S. Rodney, Cauldrons in the cosmos (University of Chicago Press, Chicago, 1988).
[2] H.J. Assenbaum, K. Langanke and C. Rolfs, Z. Phys. A 327 (1987) 461.
[3] K. Langanke and C. Rolfs, Mod. Phys. Lett. A 4 (1989) 2101.
[4] S. Engstler et al., Phys. Lett. B 202 (1988) 179.
[5] G. Blüge et al., Z. Phys. A 333 (1989) 219;
L. Bracci et al., Nucl. Phys. A 513 (1990) 316.
[6] J.B. Marion, G. Weber and F.S. Mozer, Phys. Rev. 104 (1956) 1402.
[7] W. Gemeinhardt, D. Kamke and C. von Rhöneck, Z. Phys. 197 (1966) 58.
[8] O. Fiedler and R. Kunze, Nucl. Phys. A 96 (1967) 513.
[9] H. Spinka, T.A. Tombrello and H. Winkler, Nucl. Phys. A 164 (1971) 1.
[10] J. Szabo et al., Nuclear data for science and technology, ed. K.H. Böckhoff (ECSC, Brussels, 1983) p. 956;
J. Szabo, private communication.
[11] T. Shinozuka, Y. Tanaka and K. Sugiyama, Nucl. Phys. A 326 (1979) 47.
[12] A.J. Elwyn et al., Phys. Rev. C 20 (1979) 1984.
[13] J.U. Kwon, J.C. Kim and B.M. Sung, Nucl. Phys. A 493 (1989) 112.
[14] M. Manalis and J.E. Henkel, Phys. Rev. 136 (1964) B1741.
[15] C.C. Lee, J. Korean Phys. Soc. 2 (1969) 1.
[16] C.R. McClenahan and R.E. Segel, Phys. Rev. C 11 (1975) 370.
[17] A.J. Elwyn et al., Phys. Rev. C 16 (1977) 1744.
[18] M.S. Golokov et al., Sov. J. Nucl. Phys. 34 (1981) 480.
[19] C. Rolfs and R.W. Kavanagh, Nucl. Phys. A 455 (1986) 179.
[20] J.F. Harmon, Nucl. Instrum. Methods B 40/41 (1989) 507.
[21] S. Engstler, Thesis, Universität Münster (1991), to be published.
[22] G. Raimann, Thesis, Universität Münster (1991), to be published.
[23] J.E. Monahan, A.J. Elwyn and F.J.D. Serduke, Nucl. Phys. A 269 (1976) 61.
[24] B. Kirch, Diplomarbeit, Universität Münster (1991).